

COGNITION: From Evaluation to Defense against Multimodal LLM CAPTCHA Solvers

Junyu Wang
Missouri University of Science and
Technology
Rolla, USA
jwkyx@mst.edu

Changjia Zhu
University of South Florida
Tampa, USA
changjiaz@usf.edu

Yuanbo Zhou
Missouri University of Science and
Technology
Rolla, USA
yztptn@mst.edu

Lingyao Li
University of South Florida
Tampa, USA
lingyaol@usf.edu

Xu He
Visa USA Inc.
New York, USA
xuhe3@visa.com

Junjie Xiong*
Missouri University of Science and
Technology
Rolla, USA
junjiexiong@mst.edu

Abstract

This paper studies how multimodal large language models (MLLMs) undermine the security guarantees of visual CAPTCHA. We identify the attack surface where an adversary can cheaply automate CAPTCHA solving using off-the-shelf models. We evaluate 7 leading commercial and open-source MLLMs across 18 real-world CAPTCHA task types, measuring single-shot accuracy, success under limited retries, end-to-end latency, and per-solve cost. We further analyze the impact of task-specific prompt engineering and few-shot demonstrations on solver effectiveness. We reveal that MLLMs can reliably solve recognition-oriented and low-interaction CAPTCHA tasks at human-like cost and latency, whereas tasks requiring fine-grained localization, multi-step spatial reasoning, or cross-frame consistency remain significantly harder for current models. By examining the reasoning traces of such MLLMs, we investigate the underlying mechanisms of why models succeed/fail on specific CAPTCHA puzzles and use these insights to derive defense-oriented guidelines for selecting and strengthening CAPTCHA tasks. We conclude by discussing implications for platform operators deploying CAPTCHA as part of their abuse-mitigation pipeline. Code Availability ¹.

CCS Concepts

• Security and privacy → Web application security.

Keywords

CAPTCHA security, Responsible Web AI, Multimodal Large Language Model vulnerabilities, Human-centric security design

1 Introduction

Today, visual CAPTCHA (*Completely Automated Public Turing test to tell Computers and Humans Apart*) challenges are an essential security mechanism in the modern web ecosystem. CAPTCHA has been integrated into more than 10-million commercial websites worldwide, reflecting its role as a standard security layer in online services [12]. Online services rely on CAPTCHAs to distinguish human users from automated scripts, thereby protecting registration flows, content submission portals, and valuable resources from

large-scale abuse. Their ubiquity reflects their continued importance in securing everyday online interactions.

However, the advancement of multimodal large language models (MLLMs) poses a serious threat to this web security mechanism. Unlike prior attack methods that require task-specific training data and architectures [10, 15, 22], MLLMs can jointly interpret images and natural language instructions through a unified interface, precisely the capability that modern CAPTCHAs assume only humans possess. Recent work has demonstrated that MLLMs can serve as general-purpose CAPTCHA solvers [6, 25], building on earlier efforts that evaluated multimodal models under fixed templates or curated synthetic datasets [7, 16, 26]. Meanwhile, commercial CAPTCHA-solving services, often referred to as CAPTCHA farms [24], have begun combining MLLM automation with human labor to improve throughput [1, 4, 5]. If off-the-shelf MLLMs can reliably bypass CAPTCHAs at low cost and high speed, the consequences for web security are severe: attackers could automate account creation, credential stuffing, content spam, and resource scraping at unprecedented scale.

This security concern motivates our study. Rather than merely confirming that MLLMs can solve CAPTCHAs, we ask a more critical question: *which CAPTCHA designs can still raise the bar against MLLM-based solvers?* Existing studies mostly report accuracy on narrow benchmarks while overlooking solving time, retry limits, and monetary cost that determine whether an attack is viable at scale [18, 31], and they rarely analyze why models succeed on some tasks but systematically fail on others [13]. Motivated by these gaps, we consider the following research questions:

- RQ1: How well can MLLMs solve diverse visual CAPTCHA tasks under practical constraints such as limited time and retries?
- RQ2: How do prompting strategies, such as direct prompting, optimized instructions, and few-shot demonstrations, affect solver performance across different CAPTCHA types?
- RQ3: What reasoning behaviors do MLLMs exhibit during successful and failed attempts, and what do these behaviors reveal about the challenges that CAPTCHAs pose to automated solvers?

*Corresponding author

¹<https://anonymous.open.science/r/Captcha-465E/>

challenge has three pieces of information, which we will refer to throughout the paper:

- X : one or more images shown in the CAPTCHA widget (a single picture, a grid of tiles, or a composed layout) that form the visual input to the solver;
- q : the human-readable instruction on the page (e.g., “click all squares with traffic lights”);
- y : the unique correct answer stored and checked on the server side.

Only the images X and the instruction q are visible in the browser. The ground-truth answer y is never revealed to the client; the server only returns a pass/fail signal after the user submits an answer.

Benign users simply see the CAPTCHA, solve it by hand, and continue their normal interaction with the service. The malicious users (i.e., *attacker*), in contrast, controls an automated client (or a script that drives a browser) with the goal of solving CAPTCHAs at scale so that large numbers of malicious requests can be automated. In this setting, the web service together with its CAPTCHA deployment plays the role of the *victim*.

On the client side, we assume that the attacker has full control. They can capture the images X as rendered in the browser (e.g., via screenshots or image URLs), read instruction q , and programmatically submit answers. However, the attacker cannot inspect/modify the server-side verification logic and never directly observes y .

The attacker also leverages one or more MLLMs as automated CAPTCHA solvers. These models are accessed through black-box APIs, either from commercial providers or self-hosted open-source models. For each attempt, the attacker submits the images X and a prompt derived from q , optionally enhanced with task-specific optimizations, and receives a short text answer from MLLMs. The attacker has no access to gradients, internal activations, or model parameters; the models operate strictly as off-the-shelf oracles.

3.2 Attack Strategy and Modeling Assumptions

The attacker employs several prompting regimes that mirror our experimental settings. (i) *direct* prompts that forward the original instruction q (Exp1); (ii) *optimized* prompts, where the attacker designs a task-specific template with clearer reasoning rules and output format (Exp2); and (iii) *few-shot* prompts, where labeled examples are prepended (Exp4). For each model-task-type pair, the prompt template is fixed during evaluation.

Web services typically allow users to request a new CAPTCHA after a failure, but cap the total number of attempts in a session. We therefore evaluate (Exp3) an until-correct strategy in which the attacker is permitted up to k attempts per task type. After each query, if the answer fails verification and the attempt count is still below k , the attacker requests another instance of the *same CAPTCHA type* and queries the model again; otherwise they stop. All attempts within this sequence use the same task-type-specific prompt template and differ only in the sampled instance and the MLLM model’s internal stochasticity. The attacker is willing to tolerate per-session latencies on the order of seconds to tens of seconds and moderate per-call cost, as long as the overall success rate and throughput make the attack operationally viable.

Our analysis makes the following simplifying assumptions. First, conditional on a fixed model m , task type t , prompt template, and

hyperparameters, we treat each attempt as an independent and identically distributed Bernoulli trial. This allows to model multi-attempt solving (Exp3) using standard binomial reasoning and to estimate the probability of success within k attempts from single-shot tests in Exp1 and Exp2. Meanwhile, we do *not* consider stronger capabilities such as compromising the web service, exploiting implementation bugs in the CAPTCHA widget, combining MLLMs with human CAPTCHA farms, or retraining models directly on the target CAPTCHA distribution. These are important directions but orthogonal to our focus on black-box, API-level MLLM solvers.

4 Methods and Experiments

Building on the problem formulation in Section 3, we now describe our dataset, metrics, models, and experimental protocol.

4.1 Dataset and Tasks

We conduct all experiments on the recent CaptchaWorld dataset [13], which collects visual CAPTCHAs from both real-world services and synthetic environments. The raw dataset covers 20 task types and more than 300 instances; each instance contains the image(s), a natural-language instruction, and the ground-truth answer.

In this work, we apply light-weight cleaning and standardization to enable a unified MLLM-based evaluation: we remove two task types incompatible with our pipeline, correct and align labels and metadata, and normalize answer formats. The final benchmark contains 18 task types, which we group into four task families:

- **Counting and aggregation:** Dice_Count, Dart_Count;
- **Pointing and path-based localization:** Place_Dot, Geometry_Click, Pick_Area, Misleading_Click, Click_Order, Path_Finder;
- **Grid selection and matching:** Bingo, Patch_Select, Image_Recognition, Select_Animal, Unusual_Detection, Object_Match, Image_Matching;
- **Relational and transformation puzzles:** Coordinates, Connect_Icon, Rotation_Match.

Detailed task definitions, dataset statistics, and cleaning rules are deferred to Appendix A.1.

4.2 Evaluation Metrics

We evaluate CAPTCHA solving along three key dimensions: accuracy, time cost, and finite-retry behavior.

Pass@1: For each sample, let \hat{y}_i be the answer produced by the model in its first attempt. We define

$$\text{Pass@1} = \frac{1}{N} \sum_{i=1}^N \mathbb{1}\{\hat{y}_i = y_i\}, \quad (1)$$

where N is the number of evaluation samples. We analogously compute Pass@1 per task type. Since each CAPTCHA instance has a single correct answer and the service returns only a binary pass/fail signal, Pass@1 aligns closely with how real deployments validate submissions.

End-to-end latency: For each model call, we record the end-to-end latency from sending the request to receiving a complete, parseable answer. This metric directly captures the time between submitting a CAPTCHA to the model and learning whether it passed verification.

Finite-retry behavior: Real services typically cap the number of attempts per session. To summarize behaviour under a retry budget k , we report $\text{Success}@k$, the probability that at least one attempt within k succeeds, and the expected number of attempts used. We derive these quantities from single-shot Pass@1 under a simple Bernoulli model described in Section 4.5.

4.3 Models and Inference Setup

We evaluate seven representative MLLMs from major providers, covering both closed-source flagships and strong open-source vision-language models (Table 1). For GPT-series models we consider different reasoning_effort settings (e.g., *Medium* vs. *None*) to capture the effect of explicit reasoning modes.

To ensure comparability, we abstract a unified inference interface

$$\text{Invoke}(M, X, q; \theta) \rightarrow (a, \text{meta}), \quad (2)$$

where M is the model, X the CAPTCHA image(s), q the instruction prompt, and θ shared decoding parameters (temperature, maximum output length). The returned answer a is a short text; meta contains provider-specific metadata such as token counts and timestamps.

For each task type we constrain the output format to match the ground-truth answer (e.g., a single index, a coordinate pair, or a short integer). When APIs support JSON-mode or schema enforcement we use it, otherwise we instruct the model to output JSON-only and discard responses that contain extraneous text. For an error analysis purpose, we additionally ask the model to verbalize its reasoning in additional experiments.

Table 1: Multimodal models evaluated in our study.

Provider	Model	Snapshots
OpenAI	GPT-5.1 (Medium)	2025-11-13
OpenAI	GPT-5.1 (None)	2025-11-13
OpenAI	GPT-5 (Medium)	2025-08-07
Anthropic	Claude Sonnet 4.5	2025-09-29
Google	Gemini-2.5-Pro	2025-01
Google	Gemini-2.5-Flash	2025-01
Fireworks	Qwen-3-VL-235B-A22b-Instruct	2025-09-24

4.4 Experimental Protocol

Our evaluation consists of four complementary experiments that share the same dataset and metrics but differ in prompting and retry settings.

Exp1 (original prompts): Each instance is presented with the human-facing instruction q_{orig} from the dataset. For every model and task type we perform a single invocation per sample and report Pass@1 and latency. This corresponds to directly feeding the webpage instruction to an MLLM without any prompt engineering.

Exp2 (optimized prompts): For each task type we design a task-specific prompt template q_{opt} that standardizes the instruction, clarifies rules, and imposes a strict output format. All other settings are identical to Exp1. Comparing Exp1 and Exp2 isolates the effect of task-level prompt engineering.

Exp3 (finite-retry regime): We consider an “until-correct” strategy where the attacker can attempt up to k challenges of the same

type, stopping upon the first success or when a retry cap is reached. Instead of explicitly running all such sequences, we extrapolate $\text{Success}@k$ and the expected number of calls from Exp2’s single-shot accuracy using a Bernoulli model (Section 4.5), and empirically validate this approximation on a subset of tasks.

Exp4 (few-shot guidance on hard tasks): For the hardest task types identified in Exp2, we prepend two manually verified examples as few-shot demonstrations. At inference time, the model first sees these example image–instruction–answer pairs, followed by the test instance with the same optimized instruction. All decoding parameters and parsing rules remain identical to Exp2.

4.5 Single-shot Accuracy and Finite-retry Cost

We model the finite-retry setting in Exp3 as repeated Bernoulli trials. For a fixed model m and CAPTCHA type t , all attempts use the same prompt template, decoding hyperparameters, and parsing rules, and are evaluated on instances drawn from the same dataset. Conversational memory and tool use are disabled, so randomness arises only from the sampled instance and the model’s internal sampling. Under these controlled conditions, it is natural to treat each attempt’s correctness as an independent Bernoulli trial with success probability $p_{m,t}$, which we estimate by the corresponding Pass@1 from Exp2.

Given this model, if an attacker is allowed at most k attempts on type t , the probability that at least one attempt succeeds is

$$\text{Success}@k = 1 - (1 - p_{m,t})^k,$$

and the expected attempt count under this until-correct strategy is

$$\mathbb{E}[A] = \frac{1 - (1 - p_{m,t})^k}{p_{m,t}}.$$

These quantities let us summarize, for each (m, t) , how a small retry budget amplifies single-shot accuracy and how many API calls an attacker is expected to make.

We estimate per-call monetary cost from provider price tables. Let c_{in} and c_{out} be the per-thousand-token prices for prompts and completions, and let t_i^{in} and t_i^{out} be the corresponding token counts for sample i . The cost of that invocation is

$$\text{cost}_i = \frac{t_i^{\text{in}}}{1000} c_{\text{in}} + \frac{t_i^{\text{out}}}{1000} c_{\text{out}}.$$

Multiplying the average per-call cost by $\mathbb{E}[A]$ yields an estimate of the expected cost per successful solve. For comparison, prior measurements of human CAPTCHA-solving services report roughly 80–90% one-shot accuracy, solving times of a few to tens of seconds, and market prices on the order of 0.5–2 US cents per challenge [3, 14, 15]. We use these ranges as a reference when interpreting the cost–performance trade-offs of MLLM-based solvers.

5 Experiment Results

Our results reveal a clear difficulty gap across CAPTCHA types. Recognition-oriented and low-interaction tasks, such as object selection or simple grid matching, are already solved reliably by MLLMs with high accuracy, strong performance under small retry budgets, and low per-solve cost. In contrast, tasks requiring fine-grained localization, ordering, or counting remain challenging even for the

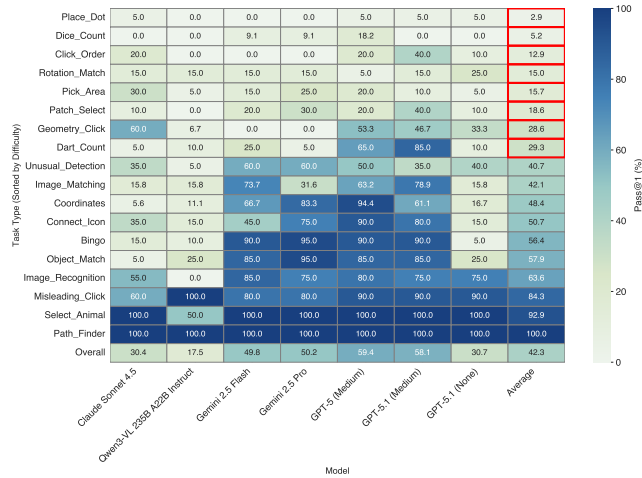


Figure 2: Heatmap of CAPTCHA task difficulty in Exp1 (original prompts). Task types (rows) are sorted by cross-model average Pass@1. Columns correspond to MLLMs, and each cell reports Pass@1 (%).

strongest models and therefore serve as the most promising directions for defense-oriented deployment. We present our empirical findings in the order of RQ1–RQ3 and discuss defense implications (RQ4) in Section 6.

5.1 RQ1: Overall Solving Capability

RQ1 asks how well MLLMs can solve diverse CAPTCHA tasks under realistic constraints such as limited time, retries, and cost. We first examine single-shot accuracy across models and task types, then connect these results to finite-retry success rates and time/cost trade-offs.

Figure 2 summarizes Exp1, where models receive the original human-facing instructions. The cross-model average Pass@1 is 42.3%, showing that MLLMs already solve a substantial fraction of CAPTCHAs even with unoptimized prompts. Strong closed-source models (GPT-5, GPT-5.1, Gemini 2.5 Pro/Flash) reach around 50–60% Pass@1, while weaker systems lag noticeably behind.

More importantly, there is a pronounced task-level hardness gap. A small set of types, including Place_Dot, Dice_Count, Click_Order, Rotation_Match, Pick_Area, Patch_Select, and Geometry_Click, have cross-model averages well below 30%, with the first six mostly below 20%. In contrast, recognition-style tasks such as Path_Finder and Select_Animal already exceed 60% on average, suggesting that they are easy targets for automated solvers.

To verify that the hardness gap is not model-specific, we examine cross-model stability. Figure 3 plots Pass@1 distributions for each task type, with a dashed line at 40% as a working CAPTCHA threshold. Tasks whose distributions lie well below this are consistently difficult across models, while those above it are reliably easy.

Exp2 replaces the prompts with task-optimized instructions. As shown in Figures 4 and 5, prompt optimization yields modest gains for strong models (e.g., GPT-5 increases from 59.4% to 60.7%, GPT-5.1 from 58.1% to 60.4%), and slightly raises the overall average from 42.3% to 43.4%. At the task level, however, the separation between

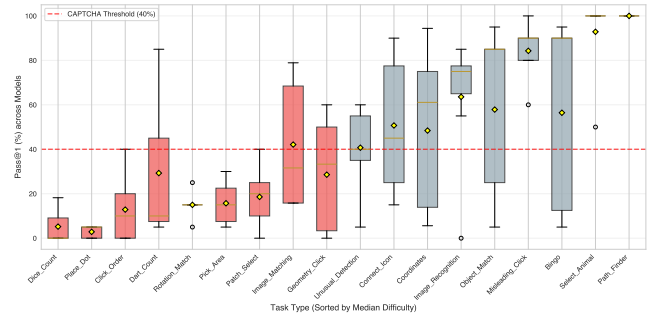


Figure 3: Cross-model Pass@1 distributions per task type in Exp1 (original prompts). Each box shows the spread across models. The dashed line marks a 40% threshold.

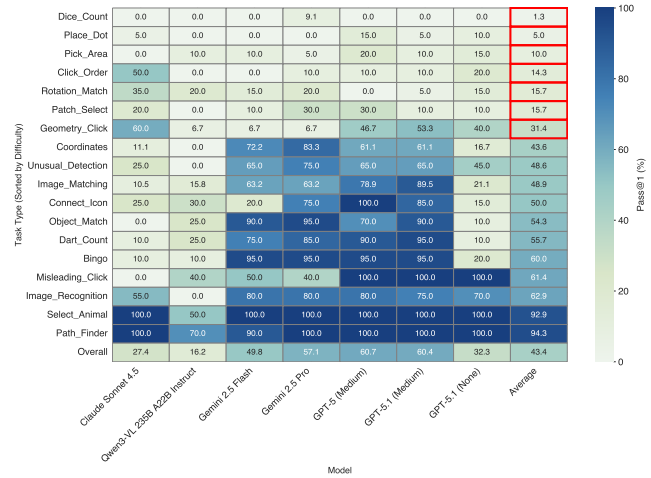


Figure 4: Heatmap of CAPTCHA task difficulty in Exp2 (optimized prompts). Task types (rows) are sorted by cross-model average Pass@1, and columns correspond to MLLMs.

easy and hard types becomes sharper: recognition-oriented tasks such as Bingo, Object_Match, Image_Recognition, and Path_Finder move further above 60%, while six types—Dice_Count, Place_Dot, Pick_Area, Click_Order, Rotation_Match, and Patch_Select—remain below 20% even after optimization. Geometry_Click improves modestly but stays around 30%.

These findings motivate a taxonomy used in the rest of the paper:

- **Broken types:** task types whose cross-model average Pass@1 exceeds 40% in both Exp1 and Exp2. This group contains recognition and simple grid-based families such as Path_Finder, Select_Animal, Misleading_Click, Image_Recognition, Bingo, Object_Match, Unusual_Detection, Image_Matching, Coordinates, Connect_Icon, and Dart_Count.
- **Borderline types:** Geometry_Click remains below 40% on average but shows clear upward trends when prompts are optimized; we conservatively treat it as effectively broken.
- **Hard types:** Patch_Select, Rotation_Match, Click_Order, Pick_Area, Place_Dot, and Dice_Count stay below 20% in

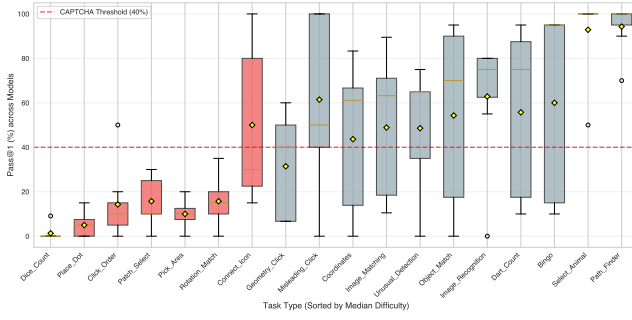


Figure 5: Cross-model Pass@1 distributions per task type in Exp2 (optimized prompts). Compared to Exp1, most recognition-style tasks rise well above the 40% threshold, while the six hard task types remain low across models.

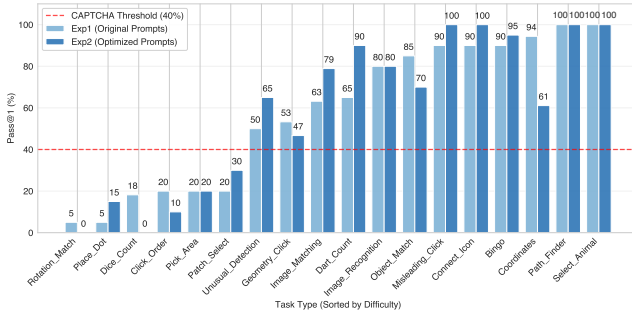


Figure 6: Per-task Pass@1 for GPT-5 (Medium) in Exp1 (original prompts) and Exp2 (optimized prompts). The dashed line at 40% marks the hardness threshold.

both experiments with minimal improvement and are our candidate robust CAPTCHAs.

We next focus on GPT-5 (Medium) as a representative strong solver, which attains the best overall performance. Figure 6 compares GPT-5’s Pass@1 under original and optimized prompts. Most recognition tasks lie well above the 40% line (often above 80%) and benefit further from optimized prompts, whereas the six hard types remain below this threshold with only small or even negative changes. This shows that prompt engineering can polish already-vulnerable tasks but does not eliminate intrinsically hard ones.

To connect single-shot accuracy with realistic retry budgets, we map Exp2 Pass@1 to Success@3 using the statistical model in Section 4.5. Figure 7 shows that once Pass@1 exceeds 40%, Success@3 quickly rises above 80%, and tasks around 60% Pass@1 already reach over 90% Success@3. All broken types fall into this regime, implying that a small retry budget suffices to make them almost always solvable. The hard types remain in the lower-left corner: with Pass@1 below 30%, their Success@3 stays moderate even with three attempts, and Dice_Count and Rotation_Match remain effectively unsolvable.

Figure 8 reports the expected number of API calls until the first success, again derived from Exp2. Broken types cluster between one and two calls on average, while the six hard tasks typically require between two and ten calls, with Dice_Count and Rotation_Match

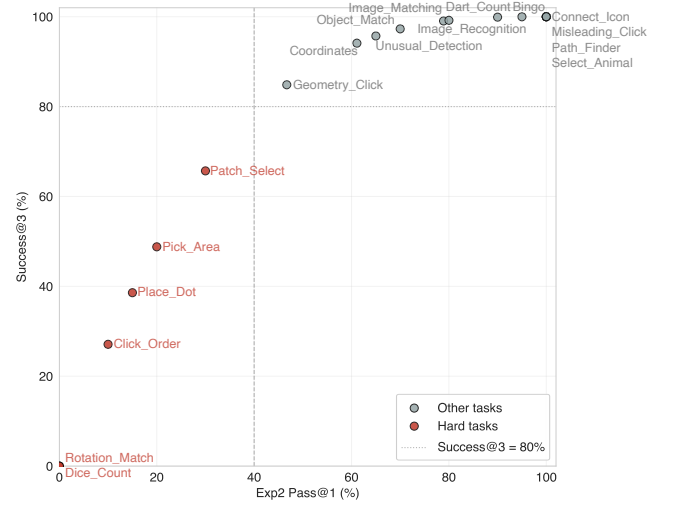


Figure 7: Mapping Exp2 Pass@1 to the finite-retry regime for GPT-5 (Medium). Each point is a task type; x-axis is single-shot Pass@1 and y-axis is the induced Success@3 under a three-attempt until-correct strategy.

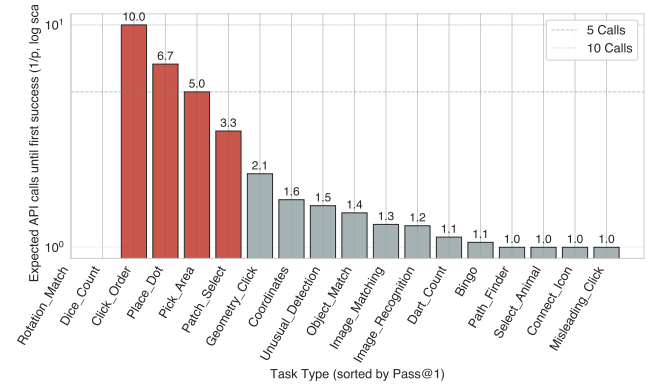


Figure 8: Expected number of API calls until the first success for GPT-5 (Medium), computed as $1/p$ based on Exp2 single-shot accuracy (log scale on the x-axis). Each point is a task type; reference lines at 5 and 10 calls highlight that hard tasks (shown in red in the plot) require significantly more calls than broken tasks.

at the upper end. Thus, even without an explicit retry cap, reliably solving hard CAPTCHAs demands substantially more queries.

We now incorporate monetary cost and latency. From an attacker’s perspective, RQ1 is not only about whether a CAPTCHA can be solved, but also whether solving it is economically and temporally viable at scale. Using the cost model in Section 4.5, Figure 9a plots per-call cost versus Pass@1, while Figures 9b and 9c show E2E latency and expected cost per successful solve. Broken types occupy the favorable region: high Pass@1, E2E times on the order of tens of seconds, and expected costs per success less than 10 cents. The six hard types sit in the opposite regime: lower accuracy, similar or higher latency, and one to two orders of magnitude higher expected

Table 2: Few-shot (Exp4) performance of GPT-5 (Medium) on the six hard task types. E2E time is computed from the average per-question latency and reported in seconds.

Task	Pass@1	Avg E2E (s)
Click_Order	0.25	31.4
Dice_Count	0.00	92.2
Patch_Select	0.00	14.0
Pick_Area	0.00	38.7
Place_Dot	0.00	38.7
Rotation_Match	0.50	45.7

cost per successful solve. Under current pricing, they are therefore economically unattractive for large-scale automated solving.

Taken together, Exp1–Exp3 and the cost/latency analysis answer RQ1: under realistic retry budgets and current API pricing, many recognition-style CAPTCHAs are already solvable cheaply and reliably, whereas the six hard task types remain both statistically and economically unattractive to automated MLLM-based solvers.

5.2 RQ2: Impact of Prompting Strategies

RQ2 asks how prompting strategies affect solver performance across CAPTCHA types. We therefore compare direct prompting (Exp1), task-optimized prompts (Exp2), and few-shot demonstrations (Exp4).

At the aggregate level, moving from original instructions to optimized prompts modestly improves overall Pass@1 for strong models (e.g., GPT-5 from 59.4% to 60.7% and Gemini 2.5 Pro from 50.2% to 57.1%). Figures 2, 4, and 6 show that these gains mainly push already-solvable recognition tasks further into the high-accuracy regime, while the six hard types remain well below the 40% threshold. Prompt engineering thus amplifies capabilities where the model is already near the decision boundary but does not change which CAPTCHA families are intrinsically difficult.

We next ask whether few-shot demonstrations can substantially close the performance gap on the hard task types. In Exp4, we prepend two labeled examples per task type to the optimized prompt and evaluate GPT-5 under otherwise identical settings (Section 4.4). Table 2 summarizes the results.

Few-shot guidance provides only limited benefit. Compared to Exp2, Click_Order improves from 10% to 25% Pass@1 and Rotation_Match from 0% to 50%, but Dice_Count, Patch_Select, Pick_Area, and Place_Dot remain unsolved. At the same time, multi-turn prompts with embedded examples substantially increase latency: the average end-to-end time per query on these six tasks is about 43.4 s, with Dice_Count exceeding 90 s. This corresponds to an average slowdown of roughly 2–3× relative to Exp2. In other words, few-shot prompting does not reliably solve hard CAPTCHAs and makes each query considerably more expensive.

Taken together, Exp1–Exp2 and Exp4 answer RQ2: task-specific prompt optimization and few-shot demonstrations improve MLLM solvers on already-vulnerable recognition CAPTCHAs, but do not qualitatively change which task families are hard. The same six hard types identified under direct prompting remain out of reach even with stronger prompting strategies.

5.3 RQ3: Which CAPTCHAs Break, Which Survive, and Why?

Combining the above results, we can now explain which CAPTCHA families current MLLMs reliably solve, which are close to being solved, and which remain comparatively robust.

Broken and near-broken types: Across Exp1 and Exp2, recognition-oriented and low-interaction tasks (e.g., object selection and coarse path finding) exhibit high Pass@1 for strong models and near-certain Success@3 with a small retry budget. These tasks require only coarse visual recognition with minimal spatial precision or multi-step reasoning, making them effectively broken under current MLLMs. Rotation_Match is an intermediate case: it remains moderately difficult with only optimized prompts, but becomes largely solvable with two few-shot demonstrations in Exp4, reducing to simple pattern matching. We therefore treat it as a near-broken type that is likely to fall completely as model capabilities improve.

Persistently hard types and shared structure: After excluding broken and near-broken CAPTCHA types, five task types remain consistently hard across models and prompting regimes: Click_Order, Place_Dot, Pick_Area, Dice_Count, and Patch_Select. Even GPT-5 with optimized prompts and few-shot examples exhibits low Pass@1, limited Success@3, and higher time and token consumption on these tasks. As discussed in Section 6, they share several structural factors: a reliance on high-precision 2D localization, multi-object binding and ordering, and counting or aggregation under clutter. These properties jointly stress aspects of spatial grounding and compositional reasoning that current MLLMs handle poorly.

Recurrent error modes: The reasoning traces logged for GPT-5 on these five task types exhibit three recurring error modes:

- *Correct reasoning, incorrect discrete answer:* the model describes the right region or counting strategy, but the final coordinate, tile index, or numeric result does not match its own reasoning.
- *Local correctness, global inconsistency:* the model correctly interprets local parts of the scene (e.g., icons or dice groups) but aggregates them inconsistently, leading to wrong click orders or off-by-one counts.
- *Overconfident approximations in spatial decisions:* the model outputs locations that are “approximately right” from a human perspective but fall outside the exact tolerance required by the verification logic.

These observations explain why only a small subset of CAPTCHA types survive our MLLM-based evaluation. Tasks that can be reduced to coarse recognition or simple matching are already broken or nearly broken, while Click_Order, Place_Dot, Pick_Area, Dice_Count, and Patch_Select continue to resist current MLLM solvers. Their shared structural weaknesses form the basis for the defense-oriented guidelines developed in Section 6.

6 Discussion

Our empirical results highlight a small set of visual CAPTCHA task types that remain consistently difficult for state-of-the-art MLLMs, even under optimized prompts, limited retries, and few-shot demonstrations. We now use these findings to answer RQ4: what strategies should web service providers adopt to deploy CAPTCHA schemes that remain effective against increasingly capable MLLM-based

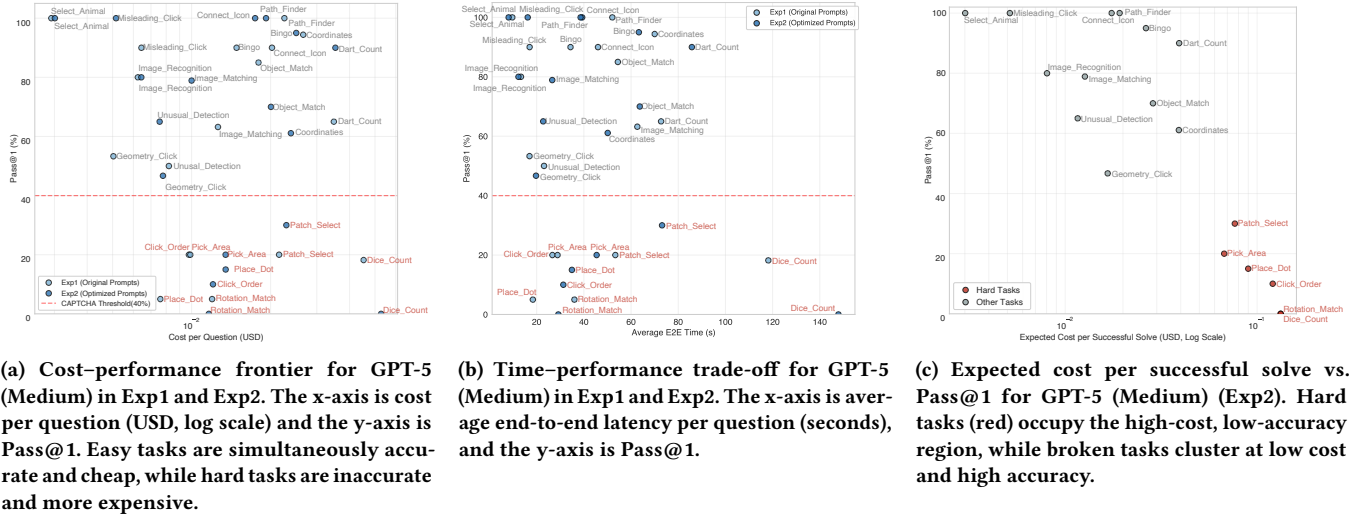


Figure 9: Cost and latency trade-offs for GPT-5 (Medium) across CAPTCHA task types.

solvers? Rather than proposing an entirely new CAPTCHA family, we extract structural *hardness factors* from the five robust task types—Click_Order, Place_Dot, Pick_Area, Dice_Count, and Patch_Select—and turn them into concrete design principles.

6.1 Hardness Factors from Robust Task Types

Fine-grained spatial localization: Across the five robust task types, the solver must localize targets on a continuous canvas rather than select from a few discrete options. The answer can be a specific point (Click_Order and Place_Dot) or a region defined by geometric or semantic cues (Pick_Area). Verification logic allows a tolerance window, but the model must still map language to precise coordinates. In practice, MLLMs often describe the correct region yet output points or areas that fall outside the acceptable zone.

Counting and aggregation beyond pattern recognition: Dice_Count and counting-based variants of Pick_Area couple visual recognition with explicit counting and light-weight arithmetic. Models frequently recognize local objects but miscount or mis-aggregate them, or make small arithmetic slips in the final answer. Humans, by contrast, are reliable at counting small sets and performing simple sums, making these tasks structurally more robust than pure recognition or binary decisions.

Stability across models and prompting regimes: Click_Order, Place_Dot, Pick_Area, Dice_Count, and Patch_Select remain hard for all evaluated models under direct prompting and optimized prompts, and they stay hard even with task-specific few-shot demonstrations. In contrast, many recognition-style CAPTCHAs are highly sensitive to prompt wording and quickly become solvable under modest prompt engineering. Robust types thus appear constrained by deeper perceptual and reasoning limitations rather than by prompt-level misunderstandings, making them better candidates for long-lived deployment.

6.2 Practical Design Guidelines

Drawing on these hardness factors, we outline several model-agnostic guidelines for deploying more robust visual CAPTCHAs.

Favor continuous-space localization over discrete choice:

Where possible, base the pass/fail decision on the user’s ability to click, drag, or draw within a continuous image, with a limited tolerance band, rather than on selecting one of a small number of buttons or tiles. Tasks in the spirit of Click_Order, Place_Dot, and Pick_Area—where a semantic instruction must be grounded into specific positions or regions—are structurally harder for current MLLMs than pre-labeled multiple-choice grids.

Couple perception with counting and simple arithmetic: Instead of asking which tiles contain a certain object, prefer tasks that require counting small objects or aggregating visual evidence into a numeric answer, as in Dice_Count or counting-based Pick_Area. Even simple arithmetic (e.g., summing small numbers) interacts poorly with current visual pipelines while being easy for humans, but counts should remain small to avoid excessive user burden.

Combine multiple hardness factors in a single challenge:

A single challenge can require users to locate several small, visually similar objects in a cluttered scene, interact with them in a prescribed order, and optionally report an aggregate quantity. Such compositions remain natural for humans when scenes are not overly crowded, but force MLLMs to solve several coupled subproblems that current architectures handle unreliably.

Preserve usability and plan for evolution:

Operators should regularly re-evaluate their schemes against up-to-date MLLMs, monitor solve rates and suspicious traffic, and be prepared to rotate or adjust templates as empirical hardness erodes.

Taken together, these guidelines translate our empirical findings into structural design principles. They cannot guarantee permanent security, but they can substantially raise the economic and technical bar for attackers relying on off-the-shelf MLLMs while preserving reasonable usability for human users.

7 Conclusions

This paper examines how modern multimodal LLMs challenge the security of visual CAPTCHAs, evaluating seven representative models across 18 real-world task types under a realistic black-box threat model that accounts for retries, latency, and cost. Our results reveal a sharp hardness gap: recognition-oriented and low-interaction CAPTCHAs are now reliably solvable, often at human-like cost and within a few retries, while a compact set of tasks requiring precise localization, cross-panel consistency, and counting remains consistently robust even under optimized prompting and few-shot demonstrations. Analysis of model reasoning traces shows that failures on these hard tasks stem from persistent weaknesses in spatial grounding and object–position binding, which informs a set of defense-oriented guidelines that emphasize continuous-space localization, perception combined with counting, and the inclusion of multiple difficulty factors within a single challenge. Overall, our findings suggest that many widely deployed visual CAPTCHAs can no longer be considered reliable bot barriers in the presence of strong MLLM solvers, and that platform operators should transition toward structurally harder task families while complementing them with broader system-level defenses.

References

- [1] 2Captcha. 2025. *Image CAPTCHA Solver — Online image CAPTCHA solving service*. <https://2captcha.com/p/image-picture-captcha-solver>. Accessed: 2025-11-20.
- [2] Ismail Akrouit, Amal Feriani, and Mohamed Akrouit. 2019. Hacking google recaptcha v3 using reinforcement learning. *arXiv preprint arXiv:1903.01003* (2019).
- [3] Elie Bursztein, Steven Bethard, Celine Fabry, John C Mitchell, and Dan Jurafsky. 2010. How good are humans at solving CAPTCHAs? A large scale evaluation. In *2010 IEEE symposium on security and privacy (SP)*. IEEE, 399–413.
- [4] CaptchaCoder. 2025. *Hybrid CAPTCHA Solving Service: API & human/OCR based service*. <https://captcha-coder.com/>. Accessed: 2025-11-20.
- [5] DeCaptcha. 2025. *CAPTCHA Decoding*. <https://www.decapthcher.com/>. Accessed: 2025-11-20.
- [6] Gelei Deng, Haoran Ou, Yi Liu, Jie Zhang, Tianwei Zhang, and Yang Liu. 2025. Oedipus: Llm-enhanced reasoning captcha solver. (2025).
- [7] Elie Dessant. 2020. Buster: Bypass CAPTCHA by filling fake audio challenges. <https://github.com/dessant/buster>. GitHub repository.
- [8] Ziqi Ding, Gelei Deng, Yi Liu, Junchen Ding, Jieshan Chen, Yulei Sui, and Yuekang Li. 2025. IllusionCAPTCHA: A CAPTCHA based on visual illusion. In *Proceedings of the ACM on Web Conference 2025 (WWW)*. 3683–3691.
- [9] Yipeng Gao, Haichang Gao, Sainan Luo, Yang Zi, Shudong Zhang, Wenjie Mao, Ping Wang, Yulong Shen, and Jeff Yan. 2021. Research on the security of visual reasoning {CAPTCHA}. In *30th USENIX security symposium (USENIX security 21)*. 3291–3308.
- [10] Pierre Laperdrix, Nataliia Bielova, Benoit Baudry, and Gildas Avoine. 2020. Browser fingerprinting: A survey. *ACM Transactions on the Web (TWEB)* 14, 2 (2020), 1–33.
- [11] Jingmeng Li, Lukang Fu, Surun Yang, and Hui Wei. 2025. MI-CAPTCHA: Enhance the Security of CAPTCHA Using Mooney Images. In *Proceedings of the AAAI Conference on Artificial Intelligence (AAAI)*, Vol. 39. 1383–1391.
- [12] BuiltWith Pty Ltd. 2025. *Websites using reCAPTCHA*. <https://trends.builtwith.com/websitelist/reCAPTCHA>. Accessed: 2025-11-20.
- [13] Yaxin Luo, Zhaoyi Li, Jiacheng Liu, Jiacheng Cui, Xiaohan Zhao, and Zhiqiang Shen. 2025. Open CaptchaWorld: A Comprehensive Web-based Platform for Testing and Benchmarking Multimodal LLM Agents. *arXiv:2505.24878 [cs.AI]* <https://arxiv.org/abs/2505.24878>
- [14] Marti Motoyama, Kirill Levchenko, Chris Kanich, Damon McCoy, Geoffrey M Voelker, and Stefan Savage. 2010. Re:{CAPTCHAs—Understanding} {CAPTCHA-Solving} services in an economic context. In *19th USENIX Security Symposium (USENIX Security 10)*.
- [15] Hoang Dai Nguyen, Karthika Subramani, Bhupendra Acharya, Roberto Perdisci, and Phani Vadrevu. 2024. C-Frame: Characterizing and measuring in-the-wild CAPTCHA attacks. In *2024 IEEE Symposium on Security and Privacy (SP)*. 277–295. doi:10.1109/SP54263.2024.00200
- [16] NopeCHA LLC. 2025. NopeCHA API Documentation. <https://developers.nopecha.com/>. Accessed: 2025-05-23.
- [17] Behzad Ousat, Esteban Schafir, Duc C. Hoang, Mohammad Ali Tofghi, Cuong V. Nguyen, Sajjad Arshad, Selcuk Uluagac, and Amin Kharraz. 2024. The Matter of Captchas: An Analysis of a Brittle Security Feature on the Modern Web. In *Proceedings of the ACM Web Conference 2024 (WWW) (WWW '24)*. 1835–1846. doi:10.1145/3589334.3645619
- [18] Andreas Plesner, Tobias Vontobel, and Roger Wattenhofer. 2024. Breaking reCAPTCHA v2. In *2024 IEEE 48th Annual Computers, Software, and Applications Conference (COMPSAC)*. IEEE, 1047–1056. doi:10.1109/compsac61105.2024.00142
- [19] Andrew Searles, Yoshimichi Nakatsuka, Ercan Ozturk, Andrew Pavard, Gene Tsudik, and Ai Enkoji. 2023. An Empirical Study & Evaluation of Modern CAPTCHAs. In *32nd USENIX Security Symposium (USENIX Security 23)*. 3081–3097.
- [20] Chenghui Shi, Shouling Ji, Qianjun Liu, Changchang Liu, Yuefeng Chen, Yuan He, Zhe Liu, Raheem Beyah, and Ting Wang. 2020. Text captcha is dead? a large scale deployment and empirical study. In *Proceedings of the 2020 ACM SIGSAC conference on computer and communications security (CCS)*. 1391–1406.
- [21] Suphannee Sivakorn, Iasonas Polakis, and Angelos D Keromytis. 2016. I am robot(deep) learning to break semantic image captchas. In *2016 IEEE European Symposium on Security and Privacy (EuroS&P)*. IEEE, 388–403.
- [22] Suphannee Sivakorn, Iason Polakis, and Angelos D. Keromytis. 2016. I’m Not a Human: Breaking the Google reCAPTCHA. In *Proceedings of the 2016 ACM Asia Conference on Computer and Communications Security (ASIACCS ’16)*. ACM, 191–202. doi:10.1145/2897845.2897847
- [23] Python Song, Luke Tenyi Chang, Yun-Yun Tsai, Penghui Li, and Junfeng Yang. 2025. Reasoning under Vision: Understanding Visual-Spatial Cognition in Vision-Language Models for CAPTCHA. *arXiv preprint arXiv:2510.06067* (2025).
- [24] Verified Visitors Threat Research Team. 2024. *CAPTCHA Farms: The Forgotten Threat in Human Verification*. <https://www.verifiedvisitors.com/threat-research/captcha-farms>. Accessed: 2025-11-20.
- [25] Xiwen Teoh, Yun Lin, Siqu Li, Ruofan Liu, Avi Sollomoni, Yaniv Harel, and Jin Song Dong. 2025. Are {CAPTCHAs} still bot-hard? generalized visual {CAPTCHA} solving with agentic vision language model. In *34th USENIX Security Symposium (USENIX Security 25)*. 3747–3766.
- [26] Theyka. 2025. Turnstile-Solver: GitHub repository for Cloudflare Turnstile bypass scripts. <https://github.com/Theyka/Turnstile-Solver>. Accessed: 2025-05-23.
- [27] Sheng Tian and Tao Xiong. 2020. A generic solver combining unsupervised learning and representation learning for breaking text-based captchas. In *Proceedings of The Web Conference 2020 (WWW)*. 860–871.
- [28] Ilias Tsingenopoulos, Davy Preuveneers, Lieven Desmet, and Wouter Joosen. 2022. Captcha me if you can: Imitation Games with Reinforcement Learning. In *2022 IEEE 7th European Symposium on Security and Privacy (EuroS&P)*. IEEE, 719–735.
- [29] Zonglin Wu, Yule Xue, Yaoyao Feng, Xiaolong Wang, and Yiren Song. 2025. MCA-Bench: A Multimodal Benchmark for Evaluating CAPTCHA Robustness Against VLM-based Attacks. *arXiv preprint arXiv:2506.05982* (2025).
- [30] Guixin Ye, Zhanyong Tang, Dingyi Fang, Zhanxing Zhu, Yansong Feng, Pengfei Xu, Xiaojiang Chen, and Zheng Wang. 2018. Yet another text captcha solver: A generative adversarial network based approach. In *Proceedings of the 2018 ACM SIGSAC conference on computer and communications security (CCS)*. 332–348.
- [31] Jiaming Zhang, Jitao Sang, Kaiyuan Xu, Shangxi Wu, Xian Zhao, Yanfeng Sun, Yongli Hu, and Jian Yu. 2020. Robust CAPTCHAs towards malicious OCR. *IEEE Transactions on Multimedia* 23 (2020), 2575–2587.
- [32] Ruijie Zhao, Xianwen Deng, Yanhao Wang, Zhicong Yan, Zhengguang Han, Libo Chen, Zhi Xue, and Yijun Wang. 2023. GeeSolver: A generic, efficient, and effortless solver with self-supervised learning for breaking text captchas. In *2023 IEEE Symposium on Security and Privacy (SP)*. IEEE, 1649–1666.

Table 3: Task types and brief descriptions in our dataset.

Task type	# inst.	Brief description
Bingo	25	Swap two cells in a 3×3 emoji grid to complete a line of identical symbols.
Click_Order	10	Click a set of icons in the same order as shown in a separate reference image.
Connect_icon	20	Choose which arrow connection matches the dotted-line pattern in the reference diagram.
Coordinates	18	Select the option where a character sits at the seat indicated in the reference image.
Dart_Count	20	Choose the dartboard whose darts add up to a given target number.
Dice_Count	11	Read a composite dice scene and output the total number of visible pips.
Geometry_Click	15	Click the specified geometric element (e.g., a letter relative to a shape).
Image_Matching	19	Match an object in the left image to the correct choice on the right.
Image_Recognition	20	In a 3×3 grid, select all images containing a specified object class.
Misleading_Click	10	Click to continue while avoiding prominently highlighted "do not click" regions.
Object_Match	20	Adjust a discrete object count until it matches the reference image.
Patch_Select	10	In a 5×5 patch grid, select all patches containing a target object.
Path_Finder	10	Choose the path that moves an object to a cross-marked destination.
Pick_Area	30	Click on the largest outlined region in a complex scene.
Place_Dot	32	Place a dot at the end of a car's path along a drawn trajectory.
Rotation_Match	48	Rotate an object so that its orientation matches a reference direction.
Select_Animal	30	In a small grid, select all cells containing the target animal (e.g., fox).
Unusual_Detection	30	Select images where an animal has a mismatched head and body.

A Appendix

A.1 Dataset Description

Our benchmark contains 378 visual CAPTCHA instances across 18 task types (see Table 3). Each instance consists of one or more images (PNG/JPG) and a structured `ground_truth.json` entry with an English prompt, a short description, and machine-interpretable labels (click coordinates, grid indices, option indices, numeric counts, or rotation angles). Click-based tasks use pixel coordinates with a small tolerance radius; grid-based tasks use zero-based row-major indices; multi-answer tasks are stored as sets or sequences.

A.2 Model API Pricing

Table 4 summarizes the token-based prices used in our cost analysis. All values are in USD per 1,000 tokens and correspond to the public pricing at the time we ran our experiments. We only account for prompt and completion tokens reported by the providers; internal "reasoning" or hidden tokens (when applicable) are not observable and are therefore excluded from our estimates.

A.3 Reasoning Trace Examples on Hard CAPTCHA Types

A.3.1 Dice_Count: Over-Counting and Inconsistent Aggregation. `Dice_Count` presents a 3×2 grid of panels, each containing several dice with pips and printed digits. The task is to "read a composite dice scene and output the total number of visible pips," i.e., the

Table 4: Token-based model pricing (USD per 1,000 tokens). "Prompt" refers to input tokens; "Completion" refers to output tokens as reported by each provider.

Model (API name)	Input	Output
gpt-5	0.00125	0.01000
gpt-5.1	0.00125	0.01000
claude-opus-4-1	0.01500	0.07500
claude-sonnet-4-5	0.00300	0.01500
gemini-2.5-pro	0.00125	0.01000
gemini-2.5-flash	0.00030	0.00250
qwen3-v1-235b-a22b-instruct	0.00022	0.00088

sum of all top faces across panels. In multiple Exp4 failures, GPT-5 systematically overestimates the total by a wide margin.

In one case (ground truth 69), the model answers 92 and explains:

"I examined the six sub-images and counted only the top faces of each die ... Subimage sums: top-left = $5 + 4 + 1 + 5$, top-middle = $2 + 2 + 4 + 3$, ... bottom-right = $3 + 5 + 7 + 7$. Adding these gives $15 + 11 + 17 + 11 + 16 + 22 = 92$."

Across four sampled items, the predicted totals are 85, 82, 90, and 92, whereas the corresponding ground truths are 69, 73, 64, and 69 (overestimation of +9 to +26). The rationales consistently emphasize that only upward faces are counted, and provide panel-wise decompositions that look internally coherent.

These traces suggest that the dominant difficulty is not the final arithmetic, but the underlying perception and grouping: the model likely misinterprets side faces as top faces, double-counts dice that appear across panels, or misreads digits under perspective distortion. Once these local misreadings are propagated into the panel sums, the final aggregation step simply preserves the error.

A.3.2 Place_Dot: Coarse Path Tracing and Endpoint Mislocalization. `Place_Dot` instances show a stylized 3D city grid with a bright green navigation path and a location pin marking the car's starting point. The instruction asks the solver to "place a dot at the end of a car's path along a drawn trajectory," with server-side verification accepting clicks within a tolerance of tens of pixels.

In several Exp4 failures, GPT-5 describes a detailed procedure for tracing the path from the pin to its terminal tip, yet chooses a point that is hundreds of pixels away from the ground truth. For one puzzle (target at (290, 235), tolerance 20 px), the model clicks (565, 895), with the following explanation:

"I identified the bright green path connected to the car pin (start) at the top-right. Tracing the single continuous ribbon through its 90-degree turns leads to the opposite end near the lower central-left area. I clicked the visual center of that squared tip."

The Euclidean distance between prediction and target exceeds 700 px. Similar patterns appear in other items (e.g., predicted (400, 690) vs. ground truth (305, 520), distance ≈ 195 px; predicted (560, 720) vs. (456, 413), distance ≈ 324 px). In all cases, the model explicitly claims to follow "only the path attached to the pin" and to click "the center of the terminal tip," but the actual coordinates clearly lie on a different segment or in a different region altogether.

This illustrates that, even when the global structure of the path is understood conceptually, the model struggles to maintain a precise, metric-consistent representation of the polyline in image space. Perspective effects and 3D shading further complicate the mapping from the verbal notion of “the end of the path” to an exact pixel location. The resulting errors are far larger than the tolerance window configured by the CAPTCHA, leading to systematic failures.

A.3.3 Click_Order: Icon Matching versus Boundary-Sensitive Localization. Click_Order consists of a reference strip showing a sequence of icons (e.g., light bulb, wheel, briefcase, globe) and a main panel where the same icons are placed at fixed positions. The solver must “click a set of icons in the same order as shown in a separate reference image,” again with a fixed tolerance radius around each icon center.

In our sampled Exp4 traces, GPT-5 generally identifies the correct semantic order and matches each reference icon to its counterpart in the main panel. Its errors arise during localization, where it approximates centers in continuous coordinate system. For example, on one item, the ground-truth centers for the four icons are

(99, 192), (384, 50), (540, 100), (242, 274),

with tolerance 40 px. The model predicts

(655, 110), (410, 260), (235, 130), (260, 400),

leading to distances of 562 px, 212 px, 307 px, and 127 px from the respective targets—well outside the allowed radius.

The corresponding reasoning emphasizes correct icon recognition and order:

“The main image shows a briefcase in the upper-left, a light bulb in the upper-right, a circular wheel near the center, and a globe in the lower-left. The reference strip shows the order: light bulb, wheel, briefcase, globe. I estimate the center of each icon and click them in that sequence.”

On other instances, the model’s clicks are visually close but still fail the threshold. For example, it clicks a key icon at (520, 95) while the ground-truth center is (493, 65) with a 40 px tolerance; the distance (≈ 40.4 px) exceeds the boundary by a small margin.

These traces show that Click_Order primarily stresses the transition from semantic symbol matching to precise 2D localization under a relatively tight tolerance. GPT-5 often “solves the puzzle in words” but fails at the final, discrete mapping from approximate centers to acceptable click coordinates.

A.3.4 Pick_Area: Largest-Region Selection under Qualitative Area Judgments. In Pick_Area, dashed curves partition the image into multiple enclosed regions, and the instruction is to “click on the largest outlined region in a complex scene.” Ground-truth labels are provided as bounding boxes for the largest region; the server accepts any click inside the corresponding box.

Across several Exp4 failures, GPT-5 provides a plausible qualitative description of the partition structure but selects a region that is not the largest and lies outside the correct bounding box. For instance, in one case the correct region occupies a box from (200, 300) to (510, 500), yet the model clicks (660, 110) and explains:

“The broadest region lies in the top-right corner, bounded by the top and right edges and a single sweeping dashed

curve to its left/bottom. I clicked near the geometric center of this largest area.”

In two other examples, the model similarly claims to have identified “the largest enclosed region” in the center-right or right-of-center portion of the image, but the chosen coordinates fall outside the ground-truth boxes, which are located elsewhere. In all cases, the failure is not a minor boundary effect: the predicted point belongs to a qualitatively different cell.

These traces indicate that GPT-5 approximates “largest area” based on coarse visual impressions of width and shape rather than precise geometric comparison. When several regions have comparable size or complex boundaries, the model’s qualitative heuristics mis-rank them, leading to consistent misclicks. Humans, by contrast, can reliably compare areas by inspecting the partition structure more meticulously.

A.3.5 Patch_Select: Example–Query Confusion in a Dense Scene. Patch_Select instances consist of a natural image overlaid with a 5×5 grid. The task is to “select all patches containing a target object” (e.g., a bridge or an hourglass). GPT-5 generally shows good object recognition on this task family, but the Exp4 few-shot traces reveal a distinctive failure pattern on a small set of hard items.

We analyze four puzzles with different targets (*bridge*, *hourglass*, *bench*, *maple leaf*), each with 3–6 positive patches. In all four, GPT-5 returns the empty set with high self-reported confidence (≈ 0.88). Strikingly, the “raw observation” segment of every trace describes the same nighttime street festival with a large moon-like installation, stalls on the right, chalk drawings on the pavement, and traffic cones. This is the few-shot demonstration image from the prompt, not the distinct test images used to label each puzzle.

For example, when the target is a *bridge* with ground-truth patches {17, 18, 21, 22, 23}, the model answers with no indices and explains:

“I scan for classic bridge cues—arched or flat spans, railings, decks or trusses crossing over water or roads. The scene shows a nighttime street festival with a large illuminated sphere, wires, storefronts, and barriers, but no continuous span with a walkable deck or supports. Therefore, no grid cells contain a bridge.”

When the target is instead a *bench* or *maple leaf*, the model reuses the same festival description, applies target-specific criteria (bench geometry, maple-leaf silhouette), and again concludes that no squares match the pattern.

Thus, the dominant error is not merely missed detections on the test images, but a task-level binding mistake: GPT-5 implicitly treats the few-shot example image as the one to solve for each new query. This example–query confusion is most prominent in Patch_Select and much rarer in other tasks such as Dice_Count or Place_Dot, and it contributes directly to the very low Pass@1 on Patch_Select under few-shot guidance.